

# CFD and Experimental Studies on Wind Turbines in Complex Terrain by Improved Actuator Disk Method

Xin Liu<sup>1</sup>, Shu Yan<sup>1</sup>, Yanfei Mu<sup>1</sup>, Xinming Chen<sup>1</sup>, Shaoping Shi<sup>1</sup>

<sup>1</sup>Huaneng Clean Energy Research Institute, Changping, Beijing 102209, China.

E-mail: [liuxin@hnceri.com](mailto:liuxin@hnceri.com)

**Abstract.** In this paper, an onshore wind farm in mountainous area of southwest China was investigated through numerical and experimental methods. An improved actuator disk method, taking rotor data (i.e. blade geometry information, attack angle, blade pitch angle) into account, was carried out to investigate the flow characteristic of the wind farm, especially the wake developing behind the wind turbines. Comparing to the classic AD method and the situ measurements, the improved AD shows better agreements with the measurements. The turbine power was automatically predicted in CFD by blade element method, which agreed well with the measurement results. The study proved that the steady CFD simulation with improved actuator disk method was able to evaluate wind resource well and give good balance between computing efficiency and accuracy, in contrary to much more expensive computation methods such as actuator-line/actuator-surface transient model, or less accurate methods such as linear velocity reduction wake model.

## 1. Introduction

Today, an improved estimation of the wake effects between wind turbines can benefit the design of a wind farm plan and siting. Industry sector gets used to and still continue to employ a number of engineering wake models for assessing the velocity deficits and power production behind single and multiple wind turbines[1]. These engineering models (e.g. Jensen and Frandsen model) are based on the analytical solution of the simplified momentum or mass conservation equations. They require the least computational time of all kinds of wake prediction models, and are occasionally capable of giving good agreement on overall efficiency of a flat terrain field.

It is extremely challenging to assess the power performance of a wind farm in complex terrain. Engineering wake models cannot be available any more in such cases. Therefore, direct rotor modelling (DRM) by CFD RANS based models or large-eddy simulation based models) is adopted to figure out complex terrain problems. It needs the largest computational time cost and exact geometry information of blades which are not acceptable for wind farm level assessment (neither flat terrain nor complex terrain), but are able to produce a complete and detailed representation of rotor dynamic flow for just a single or quite few units. Currently, DRM is regarded as the most accurate approach but also the least used in practice.

Simplifying the rotor modelling, variations of the actuator methods (i.e. actuator disk[2, 3], actuator line[4, 5] and actuator surface[6-8]) could be alternative options to DRM. There is no exact geometry of the rotor modeled in actuator methods. These geometrical parameters and aerodynamic performance are implicitly stored in tabulated airfoil data by establishing the relationships between power and thrust coefficients, or chord lengths, twist angles, attack angles, lift coefficients and drag coefficients. The specific parameters in airfoil data depend upon the selected actuator method. Through inputting this



prepared tabulated airfoil data, actuator methods can calculate relative flow velocities and the body forces in a NS solver. The advantage of actuator methods compared to DRM is twofold: First, it enables to save mesh points because boundary layers need not to be resolved. Next, it enables to represent moving boundaries by body forces, hence intrinsic dynamically problems are easily represented without having to use moving meshes[6]. Actuator line (AL) and actuator surface (AS) methods can consider the unsteady characteristic of the flow, by means of modelling individual blades and their movement over time. Although some versions of the AD model can do unsteady simulation as well, it just simplifies the disk rotating over time, and cannot distinguish the individual blade motion. Therefore, in most cases the AD methods are adopted in steady simulations. AL and AS are able to predict the intricate details of the wake dynamics, such as tip vortices. AD is a more efficient approach than AL and AS by permitting lower spatial resolutions (i.e. mesh density) and solution as a steady-state problem [9]. Depending on the available airfoil data, rotor loading may be either approximated as a constant thrust or calculated using the blade element theory[10]. The former one is the classic AD method referred to as the Froude's [11] momentum theory, which loses the detail of flow over the individual blades. The later one is the improved AD method using the blade element theory evolved by Glauert[12], which takes the tabulated airfoil data as input parameters. The AD, AL and AS methods have been compared by various researchers under different conditions and looking at various quantities, e.g. velocities at different positions in the wake, power, etc., and the results of the comparison were dependent on the quantities compared[10, 13-16]. The turbine-induced forces (e.g., thrust, lift and drag) by means of LES [17] were compared with wind tunnel measurements and demonstrated that the improved AD and AL/AS methods gave very similar results that were in good agreement with measured data whereas the results of the classical AD method deviated significantly from the measurements. When all of these problems are considered together, improved actuator disk method would give a relatively good balance between the rotor physical characteristic fidelity, the prediction precision, and calculation efficiency. Improved AD method is a powerful tool to estimate wind resources and power output efficiency in a complex terrain farm[9].

In this paper, a real wind farm with complex terrain in mountainous area of southwest China was evaluated by RANS solver along with the  $k-\omega$  turbulence model. The improved actuator disk method, taking rotor data (i.e. blade geometry information, attack angle, blade pitch angle) into account, was carried out to investigate each turbine power output and wake interaction. The rotor data is a tabulated format including chord length, twist angle, relationship between attack angles and lift/drag coefficients, pitch angles and wind speeds, in each blade section, provided by the wind turbine manufacturer. The numerical results were compared with the classic AD method and the situ measurements for two turbines with Lidar.

## **2. Numerical modelling**

The numerical simulations in the wind farm with/without actuator disks have been performed with ANSYS Fluent Program, by solving the RANS equations with a Shear Stress Transport (SST  $k-\omega$ ) turbulence model.

### **2.1. The wind farm**

The mesoscale terrain including four wind farms, as shown in Figure 1 (a), is located on a complex terrain in mountainous area of southwest China and operated by the largest energy generating company: China Huaneng Group. The wind farm has an altitude difference of about 800 m, from the lowest valley to the highest peak, and 25 km by 25 km in length and width. There are four small wind farms operated in this region. The layout of the test wind farm in this paper is in the northwest of this region, sketched in Figure 1 (b), whose the altitude range is 2400~2749 m above the sea. Thirty-three wind turbines are installed on site, with 1.5 MW of rated power at around 10.5 m/s. The rotor diameter is 82 m and the hub height is 65 m.

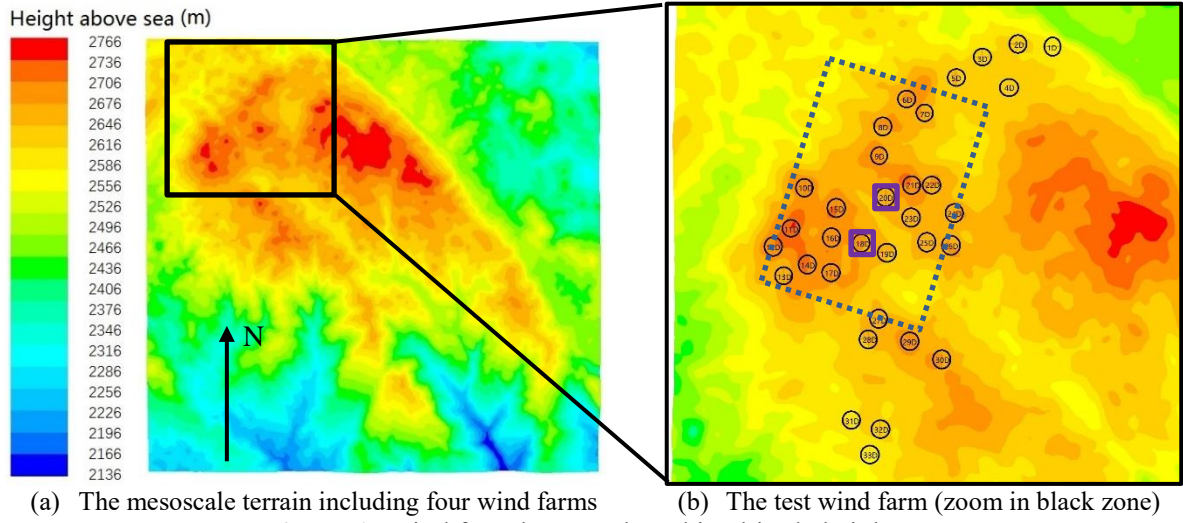


**Figure 1.** Wind farm layout, plotted in altitude height.

### 2.2. Classic actuator disk method

The classic AD method is to simply the turbine rotor as an actuator disk with uniform thrust. The rotor is modelled by porous cells instead of the swept area of the rotor. Porous cells act as a momentum absorber upon which a uniform distribution of axial force is applied [10]. The pressure drop  $\Delta p$  is calculated from the thrust coefficient curve which is given by the wind turbine manufacturer. The pressure drop through the classic AD is calculated from equation (1)[18],

$$\Delta p = \frac{T}{A} = C_T \frac{1}{2} \rho u_\infty^2 \quad (1)$$

The axial induction factor  $a$ , is defined by,

$$a = \frac{u_\infty - u_1}{u_\infty}, \text{ and } u_\infty = \frac{1}{1-a} u_1 \quad (2)$$

$u_1$  is the velocity at the hub of the rotor. From Betz's theory, if a fixed value of the thrust coefficient is assumed, the axial induction factor can be calculated as follow,

$$a = \frac{1}{2} \left( 1 - \sqrt{1 - C_T} \right) \quad (3)$$

Final, the pressure drop is obtained from

$$\Delta p = C_T \frac{1}{2} \rho \left( \frac{1}{1-a} u_1 \right)^2 \quad (4)$$

### 2.3. Improved actuator disk method

The turbine rotors are modelled as improved ADs on which body forces are imposed, described in [19-22]. Improved AD defines the blades aerodynamically as two-dimensional airfoil data. The local angles of attack and the lift and drag coefficients,  $C_L$  and  $C_D$ , are used to compute the forces acting on the blade according to,

$$f = \frac{1}{2} \rho U_{rel}^2 c B (C_L e_L, C_D e_D) \quad (5)$$

Where  $U_{rel}$  is the local relative velocity,  $c$  is the blade chord length,  $B$  indicates the number of blades,  $e_L$  and  $e_D$  are the direction of the unit vector for the lift and drag forces.

The local angle of attack is determined by the local flow angle, the twist and the pitch of the blades. The  $U_{rel}$  is obtained from the components of absolute velocity in axial  $U_{axial}$  and tangential directions  $U_\theta$ ,

$$U_{rel} = (U_{axial}, r\Omega - U_\theta) \quad (6)$$

where  $\Omega$  is the angular velocity of the rotor. The rotating speed of the turbines are determined from the inflow velocity.

If looking at a small area of the disc of differential size using cylindrical coordinates  $dA = r dr d\theta$ , the load applied in this area is given by

$$f' = \frac{f dr}{r dr d\theta} \quad (7)$$

The rotor sink terms are then subtracted from the momentum sources computed from the sum of the lift and drag forces in X, Y and Z directions by ANSYS Fluent UDF (User Defined Function).

#### 2.4. The wind measurement by lidar

Two vertically profiling, ground-based Doppler light detection and ranging (lidar) instruments was deployed in front and at back of the turbine #18, respectively. The front lidar is used to measure the velocity profile of the free stream at 224 m distance in front of the rotor. The rear lidar is used to capture the wake of the rotor at 330 m distance at the back of the rotor. The lidar locations are plotted in **Figure 2**. The lidars continuously measured the wind flow from June 5 to August 31, 2015, in vertical directions at 12 measurement heights from 45 to 155 m for the front lidar and 80 to 190 m for the rear lidar above the ground level, in steps of 10 m and sampling frequency of 1 Hz. The slopes of the ridgeline are about  $10^\circ$ , hence the lidars had to be placed at lower elevations than the base of the wind turbine.



**Figure 2.** Satellite imagery of the two lidar locations.

### 2.5. Computational domain and boundary conditions

The evaluated case in this paper was limited to a small rectangle region which is 3 kilometers long, 2 kilometers wide and 20 kilometers high, as shown in dashed frame in Figure 1 (b). The main goal of this work was to study and validate the generic behavior of the wake effect of a wind turbine in complex terrain in qualitative way rather than providing a detailed expression of the actual wind farm. The final goal of the research is to introduce the wake evaluation and AEP estimation wind turbines. Hence only 2 turbines (No. #18 and #20, see purple frame in Figure 1b) are included in the computational domain to decrease the cost of calculation. Even there are other turbines exist in this computational domain. The selection of #18 and #20 is enough to explore the impact of the wake effect. The mesh of the terrain and turbine simplified models are plotted in Figure 3. The quadrilateral mesh of the ground surface is 5 m by 5 m. The boundary layer at the ground has hexahedral grids, meshed by the first layer height of 5 meters and 10 layers in height direction with 1.2 growth ratio.

Velocity-inlet condition in ANSYS-Fluent is imposed at the inlet for pressure and velocities, pressure-outlet condition is given at the outlet, symmetry conditions are applied at the sides and top, and no slip condition with the roughness height of 0.2 m is imposed at the bottom. The rotating speed of the turbines are determined from the inflow velocities before the rotors which had been given by the turbine manufacture. The rotating speed is a function of the rotor inflow velocity, which has been given in the airfoil data and provided by the wind turbine manufacture. Fluent UDF is used to get the averaged wind speed in front the actuator disk, then to set the rotor rotating speed by checking the airfoil data. It is noted that the determination of the inlet velocity of the whole wind farm is quite tricky. Because of the complexity of the terrain, it is difficult to choose an accurate inlet velocity directly. The approach we used was as follow: first, an average wind speed in the period of one hour during a relatively steady wind flow was selected from the massive measurement database of the front lidar. Then the average speed at the elevation of 100 m was set as the target speed. The inlet velocity, which is assumed to be a logarithmic profile, was iteratively adjusted to match this target speed, as shown in Figure 4.



Figure 3. The computational mesh: AD models on actual terrain.

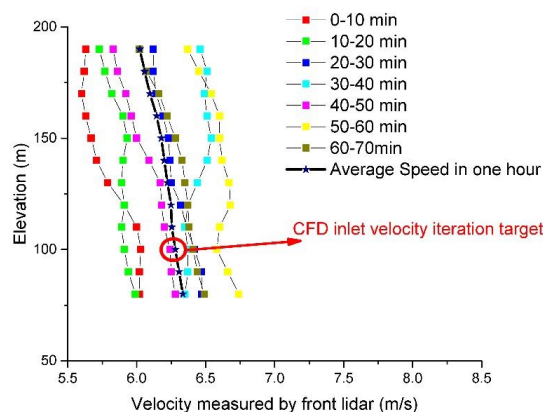
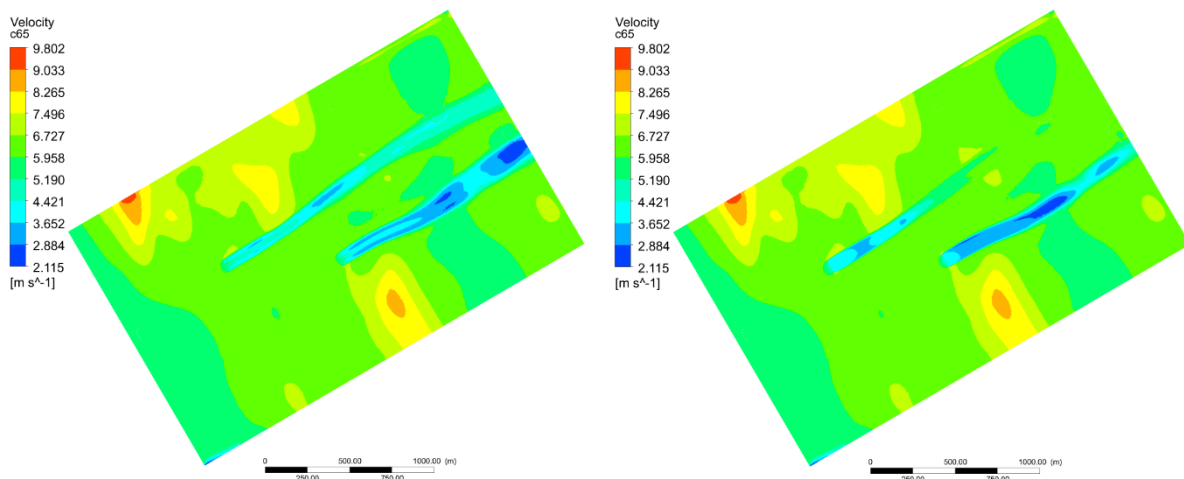


Figure 4. The reference wind speed selection.

### 3. Results

One of the major differences between complex and flat terrains is that the local velocity and pressure distribution in complex terrain highly depend upon the terrain features. The up and down of the complex terrain dramatically change wind shear, turbulence intensity, inflow angle, velocity magnitude, and so on, which in turn have important impacts on the turbine operating stability. The velocity distributions at the elevation of the turbine hub with both the classic and improved AD methods are shown in Figure 5. Wakes after the turbines (actuator disks) are clearly recognized. Unlike that in a flat terrain, the wake in complex terrain is not always straight. It changed along with the flow direction affected by mountains downstream. The wake tended to go around the mountain and pass through the valley between two mountains. The basic wake flow tracks of these two methods are almost the same, except that the improved AD predicted the wake length much longer than the classic AD.

Moreover, for cases with complex terrain, the terrain may be a more important factor for a wind farm, rather than the wake interactions. On the one hand, majority of turbines are located at the upwind sides of mountains around the peaks in prevailing wind direction. The elevations of the turbines are commonly different from each other, as well as wakes after turbines. On the other hand, because of wake flow direction change along the terrain, even if two turbines coincide in the same line of prevailing wind direction and have the same elevations, there is still the chance that the wake of the front turbine bypasses the rear one.



**Figure 5.** The velocity distributions at the elevation of the turbine hub. (left is the improved AD; right is the classic AD)

Figure 6 are the rose diagrams of the wind directions of two lidars, which were measured in one day. As it shown, the wind direction changed about  $20^\circ$  when the wind passed through the turbine rotor. At the same location of the rear lidar, the simulation result shown the wind direction changed about  $12^\circ$  (see Figure 7). This wake deflection angle was calculated as follows: the inflow direction is the free stream of the wind before the rotor, and the deflection direction is got due to the averaged velocity vector at the rear lidar location. This result indicated that CFD method was able to well predict the wake flow direction along the terrain change. The possible reason of such difference between calculation and measurement might be that the terrain model in CFD was not enough accurate and lost some details of the ground.

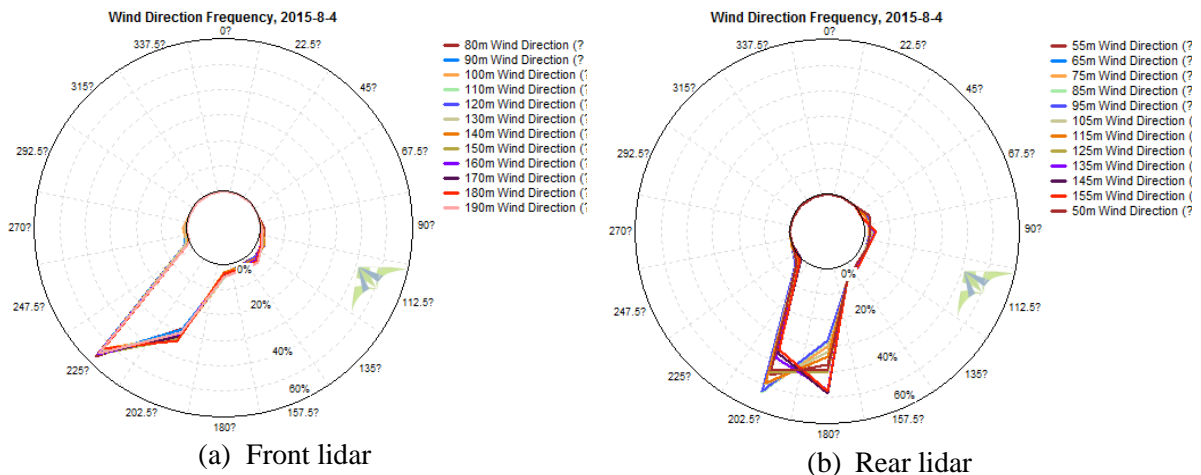


**Figure 6.** Rose diagrams of the wind direction frequency.

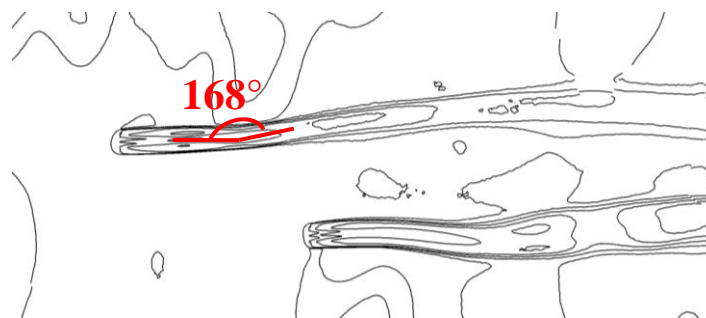


**Figure 7.** The wake deflection angle at the rear lidar location for #18.

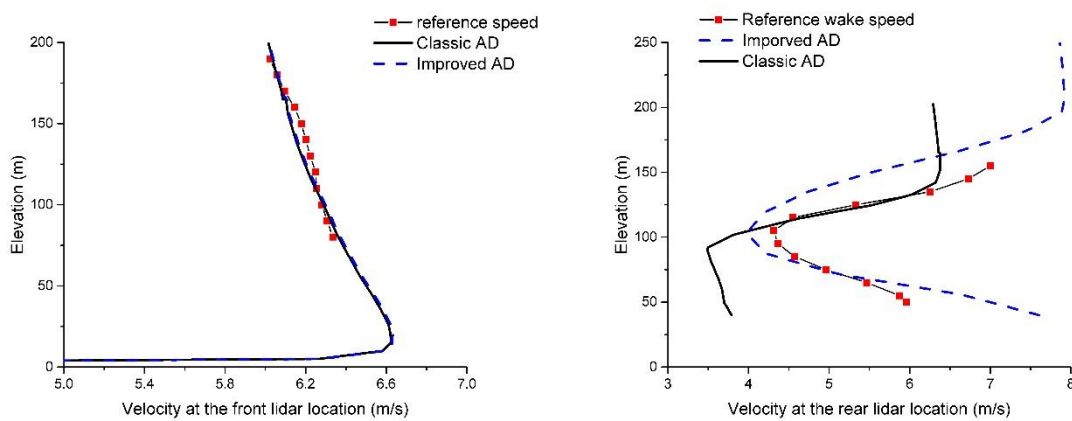


**Figure 8.** Comparison of the velocity profiles between lidars and CFD.

Before comparing velocity profiles between CFD calculations and measurements, it is noted that it is impossible to model the exact conditions of the measurements. For instance, for complex terrains it is very difficult to highlight climate effects, because multiple factors interact: orography, wakes, turbulence, wind speed, atmospheric stability [23, 24]. Meanwhile, even for measurement, it is nearly impossible to capture the totally same results, because the wind flow is extremely turbulent and results are recorded by means of time averaging method. As discussed before in Figure 4, the measurement results are carefully selected from a relatively steady wind flow. The average velocity of this period was set as the reference condition of CFD. Three different atmospheric stability, convective, near-neutral

and stable, will induce totally different velocity profiles of the free stream and wind turbine wake, as indicated by lidar data. However atmospheric stability model was not taken into account in CFD at this stage. The predicted velocity profiles of the free stream in front of the rotor were nearly the same for both improved AD and classic AD, and agreed well with measurement results (see Figure 8 left). This results were easy to understand because the AD didn't play any role in area of the rotor upstream. Simulation result of improved AD slightly over-predicted the velocity deficit after the rotor, but the shape of the profile was very similar with the measurement results. On the contrary, the results of classic AD had much larger deviation from the measurement results (see 8 right).

The negative slope of the velocity profile at the front lidar location was different from the commonly known logarithmic profile. This is due to the location of the lidar and specific terrain shape. In this case, the front lidar was placed at the upwind side of the mountain, where the up-coming wind will be accelerated near the ground.

Another advantage of the improved AD method compared with the classic AD method is that the former one is able to directly predict the power output of the turbine at any operating condition in CFD (see Figure 9). This is because the improved AD method provides blade geometry information and blade pitch angle, and the Fluent provides wind flow characteristics; Based on blade element theory, combining these factors will obtain the turbine power output. Considering the large simplification in simulation, this calculated result by improved AD seemed satisfied and be able to assess the wind farm well with turbines included.

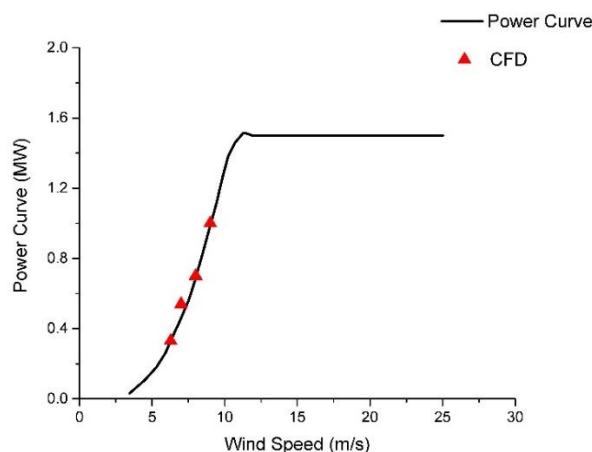


**Figure 9.** Comparison power prediction for #18 by improved AD with power curve by manufacturer.

#### 4. Conclusion

In this work, the flow characteristics of wind turbines on an onshore wind farm in mountainous area of southwest China were investigated through numerical and experimental methods. Both the classic and improved AD models have applied to simulate the presence of the rotors. Two lidars were placed in front and at back of the turbine #18, respectively to measure the inflow and wake flow. The improved AD slightly over-predicted the velocity deficit after the rotor but captured the velocity profile much better comparing to the classic AD. Moreover the terrain will change the wake developing direction which makes the behaviour of wake more complex. Generally, the improved AD model is a powerful and high-efficient tool for investigating rotor aerodynamic behavior, as well as predicting the power output of the wind turbine.

#### Acknowledgments

This work was supported by China Huaneng Group Science and Technology Fund (HNKJ15-H17).

#### References

- [1] Andersen S J, Sørensen J N, Ivanell S and Mikkelsen R F 2014 Comparison of Engineering Wake Models with CFD Simulations *Journal of Physics: Conference Series* **524** 012161

- [2] Mahmoodi E, Jafari A and Keyhani A 2015 Wind Turbine Rotor Simulation via CFD Based Actuator Disc Technique Compared to Detailed Measurement **4**
- [3] Sørensen J N, Shen W Z and Munduate X 1998 Analysis of wake states by a full - field actuator disc model *Wind Energy* **1** 73-88
- [4] Porte-Agel F, Wu Y T, Iungo V and Lu H 2011 Large-eddy simulation of atmospheric boundary layer flow through wind farms *Journal of Wind Engineering and Industrial Aerodynamics* **99** 154-68
- [5] Shen W Z, Sørensen J N and Mikkelsen R 2005 Tip Loss Correction for Actuator/Navier–Stokes Computations *Journal of Solar Energy Engineering* **127** 209-13
- [6] Shen W Z and Zhang J H 2009 The Actuator Surface Model: A New Navier–Stokes Based Model for Rotor Computations *Journal of Solar Energy Engineering* **131** 284-9
- [7] Shen W Z, Sørensen J N and Zhang J H 2007 Actuator Surface Model for Wind Turbine Flow Computations
- [8] Zhang J 2004 Numerical Modeling of Vertical Axis Wind Turbine (VAWT) *Technical University of Denmark*
- [9] Gomes V M M G C, Palma J M L M and Lopes A S 2014 Improving actuator disk wake model *Journal of Physics: Conference Series* **524** 012170
- [10] Tzimas M and Prospathopoulos J 2016 Wind turbine rotor simulation using the actuator disk and actuator line methods **753**
- [11] Froude R E 1889 On the part played in propulsion by differences of fluid pressure *Transactions Of The Royal Institution Of Naval Architects* **30**
- [12] Glauert H 1935 *Airplane Propellers*: Springer Berlin Heidelberg)
- [13] Martinez L, Leonardi S, Churchfield M and Moriarty P 2013 A Comparison of Actuator Disk and Actuator Line Wind Turbine Models and Best Practices for Their Use. In: *Aiaa Aerospace Sciences Meeting Including the New Horizons Forum and Aerospace Exposition*,
- [14] Martínez - Tossas L A, Churchfield M J and Leonardi S 2015 Large eddy simulations of the flow past wind turbines: actuator line and disk modeling *Wind Energy* **18** 1047-60
- [15] Panjwani B 2014 OffWindSolver: Wind Farm Design Tool Based on Actuator Line/Actuator Disk Concept in OpenFoam architecture. In: *Symposium on Openfoam in Wind Energy*,
- [16] Watters C S, Breton S P and Masson C 2010 Application of the actuator surface concept to wind turbine rotor aerodynamics *Wind Energy* **13** 433-47
- [17] Porteaegel F, Wu Y T, Iungo V and Lu H 2011 Large-eddy simulation of atmospheric boundary layer flow through wind farms *Journal of Wind Engineering & Industrial Aerodynamics* **99** 154-68
- [18] Crasto G and Gravdahl A R 2008 CFD wake modeling using a porous disc. In: *WindSim User Meeting*, (Tønsberg, Norway: WindSim AS)
- [19] Mozafari J and Teymour A 2014 Numerical investigation of Marine Hydrokinetic Turbines: methodology development for single turbine and small array simulation, and application to flume and full-scale reference models *Software for Computer Control* **52** 129-34
- [20] Nilsson K, Ivanell S, Hansen K S, Mikkelsen R, Sørensen J N, Breton S P and Henningson D 2014 Large - eddy simulations of the Lillgrund wind farm *Wind Energy* **18** 449-67
- [21] Lavaroni L, Watson S J, Cook M J and Dubal M R 2014 A comparison of actuator disc and BEM models in CFD simulations for the prediction of offshore wake losses *Journal of Physics: Conference Series* **524** 012148
- [22] Nilsson K 2012 Numerical computations of wind turbine wakes and wake interaction : Optimization and control. (Stockholm, Sweden: Royal Institute of Technology) p 62
- [23] Castellani F, Astolfi D, Terzi L, Hansen K S and Rodrigo J S 2014 Analysing wind farm efficiency on complex terrains *Journal of Physics: Conference Series* **524** 012142
- [24] Wharton S, Newman J F, Qualley G and Miller W O 2015 Measuring turbine inflow with vertically-profiling lidar in complex terrain *Journal of Wind Engineering and Industrial Aerodynamics* **142** 217-31